Simulated Performance of an Artificial Transmission Line Electro-Absorption Optical Modulator

M. Mbabele and C. S. Aitchison

Microwave System Research Group, Advanced Technology Institute, University of Surrey, Guildford, Surrey, GU2 5XH, UK

Abstract: **The paper shows by simulation that improved performance can be obtained from an artificial transmission line optical modulator using three MQW electro-absorption devices compared with the conventional single device configuration of the same total capacitance. The -3dBe modulation bandwidth is doubled and the return loss improved.**

I. Introduction

Electro-Absorption modulators are fabricated on heavily doped substrates and are based on the use of optical mechanisms which produce a change in the optical attenuation at the modulating frequency.

Multi Quantum Well (MQW) Electro-Absorption (EA) modulators provide a useful technique for modulating an optical carrier. They are very suitable for high bit rate optical transmission because they have the highest modulation efficiency amongst the various optical modulators [1].

We may expect an increase of the modulation bandwidth in a modulator with a number of EA devices imbedded into an artificial transmission line (ATL), having arranged that the total EA device capacitance remains invariant. Aitchison et al previously applied the ATL technique to Lithium Niobate optical modulators [2]. Our analysis together with the simulated results show that the bandwidth of the ATL EA is substantially in excess of that obtained from a simple conventional EA modulator in a 50• environment for the same total EA device capacitance. This technique also improves the return loss of the modulator.

Simulation of an ATL EA modulator using InGaAs/InAlAs MQWs enables a –3dBe bandwidth prediction for such configurations to be carried out and to be compared with the bandwidth of a single device of the same total capacitance in a 50• environment. It is found that an ATL modulator has a 3dBe bandwidth, which is larger than that of a single device since the CR time constant constraint is absent in an ATL modulator.

II. Principle of Artificial Transmission Line Optical Modulator

The bandwidth of a conventional EA modulator is restricted by the CR time constant. In order to improve the modulation bandwidth it is necessary to reduce or eliminate this effect [4]. This could be achieved by a reduction in EA device capacitance but that would reduce the modulation depth unacceptably.

An alternative approach is to use the traveling wave configuration. The CR time constant is removed by the use of a structure, which is not short compared with the modulating frequency wavelength if it is arranged that both the optical and modulating waves travel with same group velocity down the structure thereby providing the maximum modulating bandwidth. In this arrangement, a number of EA devices form the shunt elements of the ATL and the series inductors are deposited conductors.

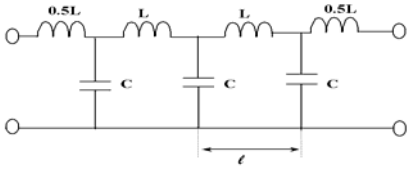

Fig. 1. Artificial transmission line equivalent circuit

A simple ATL is shown in Fig. 1, which shows the shunt capacitors, C, and the series inductors, L, both of which are lumped elements.

The principle of the ATL modulator can be conveniently illustrated by considering the electrical and optical phase velocities, V_e and V_{op}, which are given by

$$V_e = \frac{l}{\sqrt{LC}} \text{ and } V_{op} = \frac{c}{n_{op}}$$

where l is the length of each section of the ATL, c is the velocity of light in free space and n_{op} is the optical refractive index. Equating the above equations to

ensure that the electrical group and optical phase velocities are equal gives L and C in terms of n_{op}, Z_o (the characteristic impedance of the ATL), c and *l*.

$$L = \frac{n_{op} l Z_0}{c} \text{ and } C = \frac{n_{op} l}{Z_0 c}$$

The above equations can be used to calculate L and *l* for a n-section ATL for an EA device of capacitance, C. This analysis assumes negligible loss in both the EA device and the series inductor and that group delay effects in the ATL are negligible.

The calculated ATL series inductance from the above equations is 207pH for a capacitance of 88fF and separation, l, of 420µm for a 50• line. The EA device length is 105µm. These parameters are compatible with current device fabrication technology [5].

II. EA Device Modeling

A typical single device InGaAs/InAlAs MQW device is shown in Fig. 2 [3]. It consists of ten 10nm thick InGaAs wells separated by 5nm thick InAlAs barriers. The InP mesa is 1µm wide with a height of about 5.6µm. This structure was simulated using Silvaco semiconductor modeling software, ATLAS, to obtain the shunt admittance and capacitance values as a function of frequency. The shunt values were transformed to the series equivalent values of Fig. 3a.

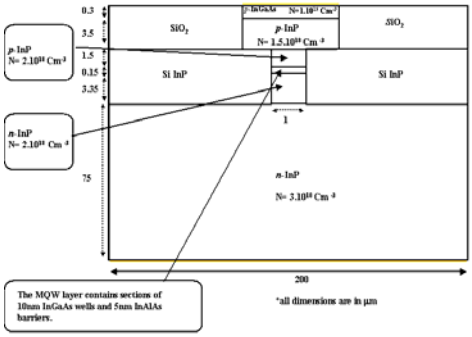

Fig. 2. Cross section of the MQW EA optical device

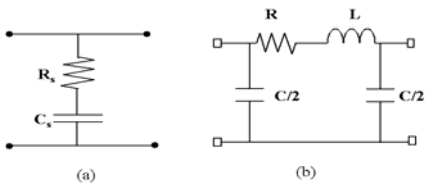

Fig.3 Series equivalent circuit of the EA device (a) and of lumped equivalent of the inductance (b)

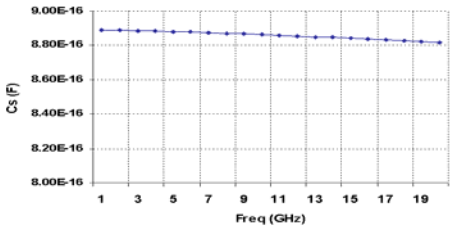

Fig. 4. EA series capacitance variation with frequency

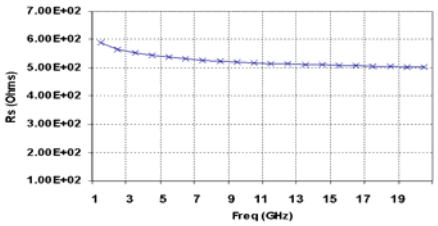

Fig. 5. EA series resistance variation with frequency

Fig. 4 shows the variation of the simulated series capacitance, C_s, with frequency for a device length of 1µm at a bias of –2V illustrating a negligible variation of C_s with frequency. Fig. 5 shows the variation of the series resistance, R_s, with frequency for a device length of 1µm at a bias of –2V for a device length of 1µm illustrating that above 2GHz the resistance is substantially constant.

These results correspond to a total capacitance per unit length of 0.088pF/mm and a resistivity of 0.52Ω-mm. The series resistance and capacitance values are used to predict the –3dBe EA bandwidth.

III. Inductance Modeling

The inductance is deposited on a substrate, which comprises a thin SiO_2 layer of 3µm immediately beneath the conductor, followed by a 5µm semi insulating InP layer and then a thick 80µm n-doped layer of InP with a resistivity of $2.7.10^{-3}$Ω-cm as shown in Fig. 6.

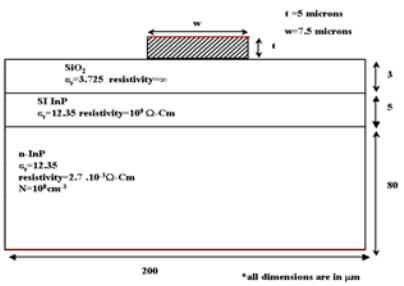

Fig. 6. Cross-section of inductance and substrate

Simulation of an inductance of cross-section of 30µm x 5µm with the required length was performed using Sonnet which yields frequency dependent s-parameters. The resulting component values of the equivalent circuit shown in Fig. 3b were derived using the Agilent ADS simulator.

The inductance, and resistance values as a function of frequency are shown in Figs. 7 and 8 respectively, illustrating a small reduction of inductance with frequency, and a resistance which rises significantly with frequency. This loss is higher than previously reported for a simpler related structure [6]. The capacitance is frequency invariant.

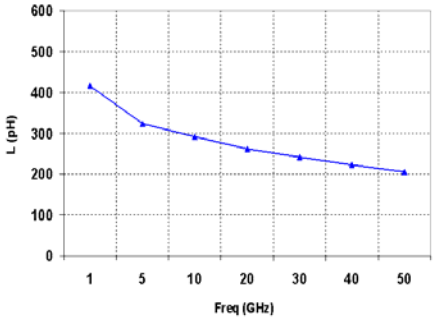

Fig. 7. Series inductance variation with frequency

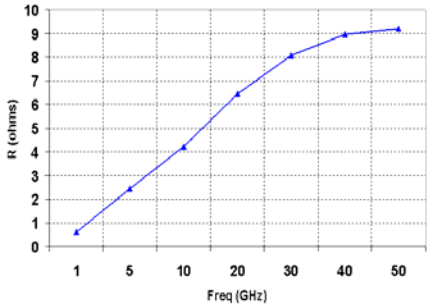

Fig. 8. Series resistance variation with frequency

IV. ATL EA Modulator Performance

The circuit of Fig. 9 was used to simulate the frequency response of the modulator. Voltage controlled current generators with a time delay to represent the optical group delay are associated with each node of each section. The microwave group delay and magnitude of voltage across each node were obtained from ADS.

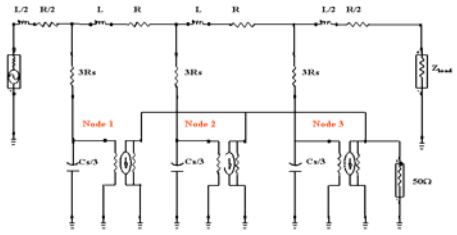

Fig. 9. Simulated equivalent circuit of the ATL EA modulator

Since the ATL EA optical modulators comprises three active sections of 100µm length, the corresponding series capacitance and resistance values for the individual section are 88fF and 5.2Ω.

Fig. 10 shows the individual modulating voltage magnitudes at node 1, 2 and 3 as a function of frequency showing an increasing reduction in voltage as the modulating signal passes down the ATL. Fig. 11 shows the signal group delay as a function of frequency showing the effect of the ATL cut-off frequency.

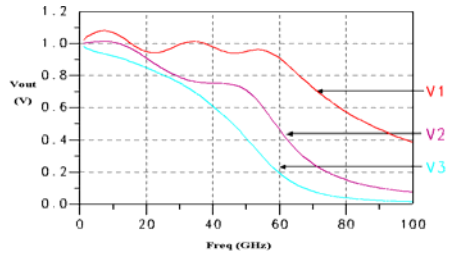

Fig. 10. Simulated voltage magnitudes at nodes 1, 2 and 3

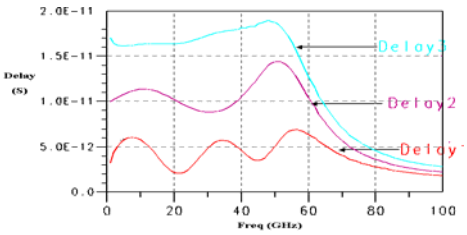

Fig. 11. Simulated group delay at nodes 1, 2 and 3

The total modulator response is obtained by combining vectorially the modulating voltage magnitude as a function of frequency including the effects of group delay variation with frequency.

This normalized modulator response is given by

$$\frac{1}{N}\sqrt{\left(\sum_{n=1}^{N}|V_n|\cos[\omega\tau'_n]\right)^2+\left(\sum_{n=1}^{N}|V_n|\sin[\omega\tau'_n]\right)^2}$$

where N is the number of sections, V_n is the voltage magnitude at node n, ω is the modulating frequency and τ_n' is the difference between the optical and microwave group delay at node n.

This response is shown as a function of frequency in Fig. 12. The –3dBe bandwidth corresponds to a total normalized response of 0.707 and the bandwidth is thus 41GHz. The corresponding modulator return loss is shown in Fig. 13 and is better than –16.6dB up to 40GHz.

These results are for an unoptimised ATL EA structure. Optimisation of the ATL inductances increases the –3dBe bandwidth response of the modulator. Furthermore, the use of an optimised terminating load can increase the bandwidth in exchange for degraded return loss performance.

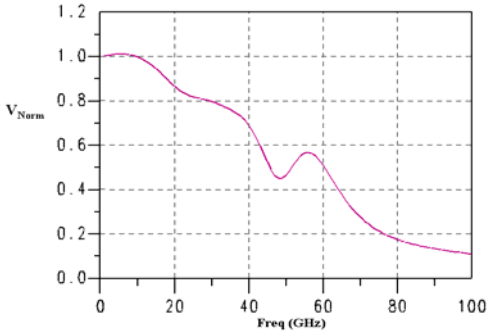

Fig. 12. Simulated overall response of the ATL EA optical modulator

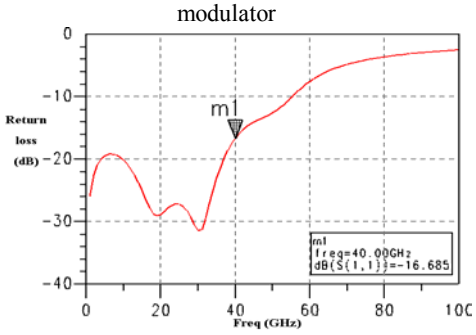

Fig. 13. Simulated return loss of the ATL EA modulator

It is helpful to predict the performance of a single EA device modulator of total capacitance 264fF and series resistance 1.75Ω in a 50Ω environment for comparison purposes. Fig 14 shows the overall modulator response of this configuration illustrating a predicted bandwidth of 23GHz The corresponding return loss is also shown in Fig. 14 demonstrating –5dB at 20GHz. This shows an increase of about 100% from a single device typical product measurement of 20GHz bandwidth [3] to a predicted 41GHz for the ATL EA device, both terminated in 50•.

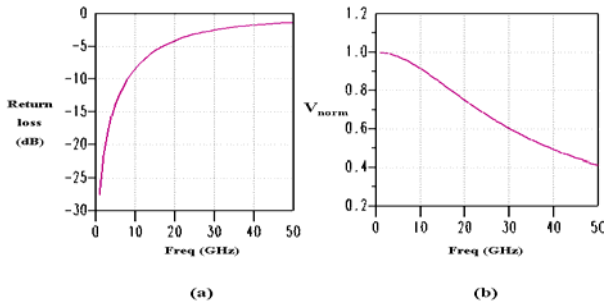

Fig. 14. Simulated input return-loss and overall response of single EA modulator.

V. Conclusions

The performance of a three-section ATL modulator using QW EA devices has been simulated and compared with the corresponding modulator in a 50Ω environment using one EA device of the same total capacitance to that of the three sections ATL structure.

Both the EA device and interconnecting inductors are simulated and the results used to predict the –3dBe bandwidth and return loss. The technique improves the single EA device bandwidth of 23 GHz with return loss of –5 to 41GHz with a return loss of –16.6dB for the three-device ATL modulator, demonstrating the benefits of the ATL arrangement.

Acknowledgement

The contribution of Dr D Moodie and his colleagues at the Corning Research Centre, Martlesham is gratefully acknowledged

References

[1] Tatemi et al, "Ultra-High Speed MQW electro-absorption optical modulators with integrated waveguides", *Journal of Lightwave Technology*, Vol. 14, No. 9, pp. 2026-2034, September 1996.

[2] Liang, J Y and Aitchison, C S, "The performance of a 10Gbits/s artificial transmission line $LiNbO_3$ optical modulator on coplanar waveguide", *Microwave Photonics '97 Technical Digest*, pp. 135-138, Sept 1997.

[3] Moodie, D G et al, "Discrete electro-absorption modulators with enhanced modulation depth", *Journal of Lightwave Technology*, Vol. 14, No. 9, pp. 2035-2043, Sept 1996.

[4] Li, G L et al, " Ultrahigh-speed travelling wave electroabsorption modulator-design and analysis", *IEEE Trans. MTT*, vol. 47,No.7, pp.1177-1183, July 1997.

[5] Moodie, D G et al, "Low polarization sensitivity electroabsorption modulators for 160Gbit/s networks", *Electr. Letts*, Vol. 33, No. 24, pp. 2068-2069, Nov 1997.

[6] Mbabele, M and Aitchison C S, “The predicted performance of an ATL electro-absorption optical modulator”, *Proc. 31st EuMC*, Workshop on Advances in Photonics Technologies for Microwave Applications, Milan, September 2002.